Consequences of Nuclear Electron Capture in Core Collapse Supernovae

W. R. Hix,[1,2,3] O. E. B. Messer,[1,2,3] A. Mezzacappa,[2] M. Liebendörfer,[4,1,2] J. Sampaio,[5] K. Langanke,[5] D. J. Dean,[2] and G. Martínez-Pinedo[6,7]

[1]*Department of Physics and Astronomy, University of Tennessee, Knoxville, Tennessee 37996-1200, USA*
[2]*Physics Division, Oak Ridge National Laboratory, Oak Ridge, Tennessee 37831-6354, USA*
[3]*Joint Institute for Heavy Ion Research, Oak Ridge National Laboratory, Oak Ridge, Tennessee 37831-6374, USA*
[4]*Canadian Institute for Theoretical Astrophysics, Toronto, ON M5S 3H8, Canada*
[5]*Institute of Physics and Astronomy, University of Århus, DK-8000 Århus C, Denmark*
[6]*Institut d'Estudis Espacials de Catalunya, E-08034 Barcelona, Spain*
[7]*Institució Catalana de Recerca i Estudis Avançats, Lluís Companys 23, E-08010 Barcelona, Spain*

(Received 25 April 2003; published 14 November 2003)

The most important weak nuclear interaction to the dynamics of stellar core collapse is electron capture, primarily on nuclei with masses larger than 60. In prior simulations of core collapse, electron capture on these nuclei has been treated in a highly parametrized fashion, if not ignored. With realistic treatment of electron capture on heavy nuclei come significant changes in the hydrodynamics of core collapse and bounce. We discuss these as well as the ramifications for the postbounce evolution in core collapse supernovae.

DOI: 10.1103/PhysRevLett.91.201102 PACS numbers: 97.60.Bw, 23.40.–s, 26.50.+x

Core collapse supernovae are among the most energetic events in the Universe, emitting 10^{46} J of energy, mostly in the form of neutrinos. These explosions mark the end of the life of a massive star, the formation of a neutron star or black hole, and play a preeminent role in the cosmic origin of the elements. With the formation of an iron core in a massive star (containing the maximally bound iron and neighboring nuclei), thermonuclear energy is no longer available to slow the inexorable contraction that results from a star's self-gravity. Once this cold iron core grows too massive to be supported by the pressure of degenerate electrons, core collapse ensues. In the inner region of the core, this collapse is subsonic and homologous, while the outer regions collapse supersonically. When the inner core exceeds nuclear densities, it stiffens, halting the collapse. Collision of the supersonically infalling outer core with this stiffened inner core produces the bounce shock, which initially drives outward the outer layers of the iron core. However, this bounce shock is sapped of energy by the escape of neutrinos and nuclear dissociation and stalls before it can drive off the envelope of the star (see, e.g., [1,2]). The intense neutrino flux, which is carrying off the binding energy of the proto-neutron star (PNS), heats matter between the neutrinospheres and the stalled shock. In the neutrino reheating paradigm, this heating reenergizes the shock, which drives off the concentric layers of successively lighter elements that lie above the iron core, producing the supernova.

Unfortunately, simulations exploring the neutrino reheating paradigm often fail to produce explosions. The failure of recent spherically symmetric multigroup Boltzmann simulations [3–5] to produce explosions has removed incomplete neutrino transport as a potential cause of this failure. Models that break the assumption of spherical symmetry have achieved some success, either by an increase in the neutrino luminosity due to fluid instabilities within the proto-neutron star [6] or by enhancement of the efficiency of the neutrino heating by large scale convection behind the shock [7–9]. The PNS instabilities are driven by lepton and entropy gradients, while convection behind the shock originates from gradients in entropy that result from the stalling of the shock and grow as the matter is heated from below. However, even with such enhancements, explosions are not guaranteed [10–12]. A third potential cause of the failure to produce explosions in numerical models is incomplete or inaccurate treatment of the wide variety of nuclear and weak interaction physics that is important to the supernova mechanism. Once the supernova shock forms, emission and absorption of electron neutrinos and antineutrinos on the dissociation-liberated free nucleons are the dominant processes. However, during core collapse, electron capture on nuclei plays an important and, as we demonstrate, dominant role by significantly altering the electron fraction and entropy, thereby determining the strength and location of the initial supernova shock, as well as the entropy and electron fraction profiles throughout the core. As a result, improvements in the treatment of electron capture alter the initial conditions for the entire postbounce evolution of the supernova.

Calculation of the rate of electron capture on heavy nuclei in the collapsing core requires two components: the appropriate electron capture reaction rates and knowledge of the nuclear composition. The inclusion of electron capture within a multigroup neutrino transport simulation adds an additional requirement: information about the spectra of emitted neutrinos. Unlike stellar evolution and supernova nucleosynthesis simulations, wherein the nuclear composition is tracked in detail via a reaction

network [13,14], in simulations of the supernova mechanism, the composition in the iron core is calculated by the equation of state assuming nuclear statistical equilibrium (NSE). Typically, the information on the nuclear composition provided by the equation of state is limited to the mass fractions of free neutrons and protons, α particles, and the sum of all heavy nuclei, as well as the identity of an average heavy nucleus, calculated in the liquid drop framework [15]. In most recent supernova simulations (see, e.g., [4,8,16]), the treatment introduced by Bruenn [17] is used. This prescription treats electron capture on heavy nuclei through a generic $0f_{7/2} \rightarrow 0f_{5/2}$ Gamow-Teller resonance [18] in the average heavy nucleus identified by the equation of state. Because this treatment does not include additional Gamow-Teller transitions, forbidden transitions, or thermal unblocking (see [19]), electron capture on heavy nuclei ceases when the neutron number of the average nucleus exceeds 40. As a result, electron capture on protons dominates the later phases of collapse.

As a major advance over this simple treatment of nuclear electron capture, we have developed a treatment based on recent shell model electron capture rates from Langanke and Martínez-Pinedo (LMP) [20] for $45 < A \leq 65$ and 80 reaction rates from a hybrid shell model-RPA calculation (LMS) [19,21] for a sample of nuclei with $A = 66$–112. For the distribution of emitted neutrinos, we use the approximation described by Langanke *et al.* [22]. To calculate the needed abundances of the heavy nuclei, a Saha-like NSE is assumed, including Coulomb corrections to the nuclear binding energy [23,24], but neglecting the effects of degenerate nucleons [25]. This NSE treatment has been used in prior investigations of electron capture in thermonuclear supernovae [26]. We use the combined set of LMP and hybrid model rates to calculate an average neutrino emissivity per heavy nucleus. The full neutrino emissivity is then the product of this average and the number density of heavy nuclei calculated by the equation of state. With the limited coverage of rates for $A > 65$, this approach provides the most reasonable estimate of what the total electron capture would be if rates for all nuclei were available. This averaging approach also makes the rate of electron capture consistent with the composition returned by the equation of state, while minimizing the impact of the limitations of our NSE treatment. A more detailed description of our method, including tests of some assumptions made, will be presented in a forthcoming article [27].

Simulations of the collapse, bounce, and postbounce evolution of a 15 $M_\odot$ model [28] were carried out using the fiducial Bruenn prescription for electron capture on nuclei and our LMP + LMS treatment with our fully general relativistic, spherically symmetric AGILE-BOLTZTRAN code. In these simulations, it is employed using the equation of state of Lattimer and Swesty [15], six-point Gaussian quadrature to discretize the neutrino angular distributions, and 12 energy groups to discretize the neutrino spectra between 3 and 300 MeV.

Our improved treatment of nuclear electron capture has two competing effects. In lower density regions, where the average nucleus is well below the $N = 40$ cutoff of electron capture on heavy nuclei, the Bruenn parametrization results in more electron capture than the LMP + LMS treatment. This is similar to the reduction in the amount of electron capture seen in stellar evolution models [28] and thermonuclear supernova models [26] when earlier parametrized rates [29] are replaced by shell model calculations. In denser regions, the continuation of electron capture on heavy nuclei alongside electron capture on protons results in more electron capture in the LMP + LMS case. The results of these competing effects can be seen in the upper pane in Fig. 1, which shows the distributions of electron fraction, entropy, density, and velocity throughout the core at bounce (maximum central density).

In addition to the marked reduction ($\sim$10%) in the electron fraction in the interior of the PNS, the improved treatment of electron capture also results in an $\sim$20% reduction in the mass of the homologous core, consistent with the analysis that the size of the homologous core is proportional to the square of the mean trapped lepton fraction $\langle Y_l^2 \rangle$ at core bounce [30]. At bounce, this change in the homologous core manifests itself as a reduction in the mass interior to the formation of the shock from 0.57 $M_\odot$ in the fiducial case to 0.48 $M_\odot$ in the LMP + LMS case, as is evident in the lower pane in Fig. 1. In the LMP + LMS case there is also an $\sim$15% reduction in the

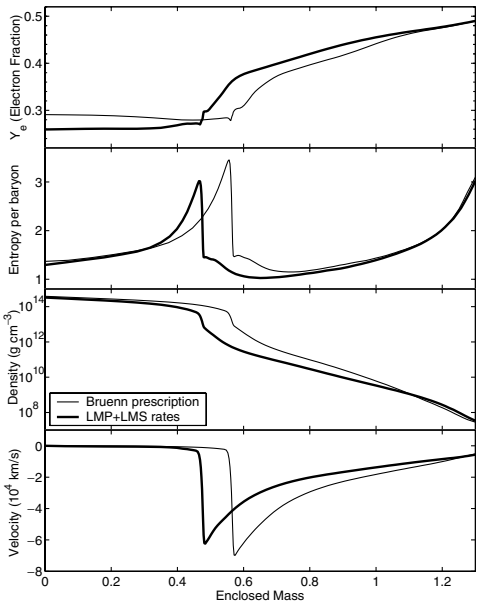

FIG. 1. The electron fraction, entropy, density, and velocity as functions of the enclosed mass at the beginning of bounce for a 15 $M_\odot$ model. The thin line is a simulation using the Bruenn parametrization, while the thick line is for a simulation using the LMP and hybrid reaction rate sets.

central density and an ~5% reduction in the central entropy at bounce, as well as an ~15% smaller velocity difference across the shock.

If the principle effect of our improvement in the treatment of electron capture on nuclei were to launch a weaker shock with more of the iron core overlying it, this improvement would make a successful explosion more difficult. However, these improvements in nuclear electron capture also alter the behavior of the outer layers which play an important role in the ultimate fate of the shock. The lesser neutronization in the outer layers slows the collapse of these layers, which further diminishes the growth of the electron capture rate by reducing the rate at which the density increases. These changes are clearly apparent in regions above the shocks in Fig. 1; for example, reductions of a factor of 5 in density and 40% in velocity are evident in the vicinity of 0.8 $M_\odot$. Such changes reduce the ram pressure opposing the shock, easing its outward progress. In these spherically symmetric models, these improvements allow the shock in the LMP + LMS case to reach 168 km, relative to 166 km in the fiducial case, in spite of the greater mass overlying the shock when it was launched and the greater loss of energy to the neutrino burst (see Fig. 2).

As mentioned earlier, changes in the electron capture rates also lead to changes in the core fluid gradients that may, in turn, drive fluid instabilities that are potentially important to the supernova mechanism. Within the inner 50 km, the entropy and lepton fraction gradients found in the LMP + LMS model are considerably different from those found in the fiducial model. Consequently, the more accurate treatment of electron capture may significantly alter the location, extent, and strength of proto-neutron star convection, or other potential fluid instabilities, in the core. This provides an excellent example of the coupling of convective behavior to radiative and nuclear processes and must be further investigated in the context of future multidimensional models.

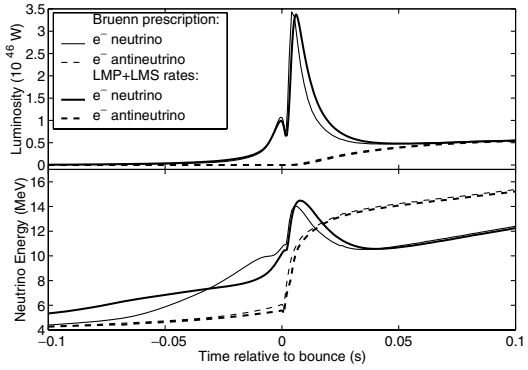

FIG. 2. The neutrino luminosity and root-mean-square energy (at 500 km) as a function of time from bounce for a 15 $M_\odot$ model. The thin lines show this evolution for a simulation using the Bruenn parametrization, while the thick lines show this evolution for a simulation using the LMP + LMS rates. The solid lines correspond to electron type neutrinos; the dashed lines correspond to electron type antineutrinos.

Figure 2 shows the luminosity and mean energy of the emitted electron neutrinos and antineutrinos between 100 ms before bounce and 100 ms after bounce. Clearly evident in the luminosity is a slight delay (2 ms) in the prominent "breakout" burst caused by the deeper launch of the shock in the LMP + LMS case. Over the first 50 ms after bounce, the LMP + LMS model emits ~15% more energy than the fiducial model, with a slightly lower luminosity at later times. This is largely the result of differences in the mean electron neutrino energy, which is as much as 1 MeV higher over the first 50 ms in the LMP + LMS case, but lower thereafter. This results from the neutrinospheres in the LMP + LMS model occurring in deeper, hotter layers for the first 50 ms, but cooler layers at later times.

The differences in the neutrino spectrum during collapse, when electron capture on nuclei dominates, are larger than those described after bounce. For low densities, where capture on nuclei dominates in the Bruenn prescription as well, the approximate reaction Q value derived from the free neutron and proton chemical potentials dramatically underestimates the Q value, resulting in a much lower mean neutrino energy. As captures on protons begin to compete with captures on nuclei in the Bruenn prescription, the mean neutrino energy grows rapidly because of the higher Q value for capture on protons. It exceeds that found in our LMP + LMS model by as much as 2 MeV in the 30 ms just before bounce. This latter effect was anticipated by Langanke *et al.* [19], who also demonstrated that nuclear electron capture should dominate that on protons because the much larger number of heavy nuclei more than compensates for the larger capture rate on free protons, at least for the conditions found in models resulting from the Bruenn prescription. These self-consistent models unequivocally show that this is correct. At the onset of collapse, there are roughly 1000 heavy nuclei per proton in the inner layers of the core. In our fiducial model this ratio declines rapidly, reaching values less than 100 by the time the central density is 10^{11} g cm^{-3} and roughly 10 by the time the central density is 10^{13} g cm^{-3}. In the LMP + LMS model, the reduced electron fraction and entropy keep this ratio near 1000 until the central density exceeds 10^{12} g cm^{-3}, reaching 50 around a central density of 10^{13} g cm^{-3}. As a result, in the regime where Y_e experiences the largest changes (10^{11-13} g cm^{-3}), the dominance of heavy nuclei is increased by a factor of 5–30, cementing the dominance of nuclear electron capture.

To implement these simulations, we have made approximations to all three components of the calculation of electron capture in core collapse supernovae. Each of these requires further improvement. Removing the averaging of electron capture rates requires better coverage of electron capture on nuclei with $A > 65$, by hybrid and approximate methods [31] in the near term, but

ultimately by finite temperature shell model calculations vetted by experimental determinations of ground state strength distributions. These reaction rates must cover the full thermodynamic range of interest in supernovae (temperatures of 1–100 GK and densities from 10^5–10^{14} g cm^{-3}) and must also address the need for the emitted neutrino spectra. Detailed tracking of the nuclear composition is also necessary, in a form that retains the consistent transition to nuclear matter afforded by current schemes [15] while allowing for accurate calculation of the rate of electron capture on heavy nuclei and, ultimately, for detailed nucleosynthesis.

We have demonstrated that supernova simulations with a modern treatment of electron capture differ significantly from previous models, which employed more parametrized treatments. Though this improved model still fails to produce an explosion in the spherically symmetric case, the differences are quite striking. The initial mass behind the shock when it is launched is reduced by 20%, with significantly (~10%) lower central densities, entropies, and electron fractions in this region. Over the first 50 ms after bounce, the neutrino luminosity is boosted by ~15% with the mean electron neutrino energy increased by ~1 MeV. In spite of an initially weaker and deeper shock and larger neutrino energy loss, reduced electron capture in the outer layers slows their collapse, allowing the shock to reach a maximum radius that is slightly larger. Furthermore, the lepton and entropy gradients in the core differ significantly. Because these gradients drive PNS convection and other potential instabilities in the core, the location and strength of such instabilities may be significantly different than heretofore thought.

The authors acknowledge helpful conversations with J. Beacom and H.-T. Janka. The work has been partly supported by NASA under Contract No. NAG5-8405, by the National Science Foundation under Contract No. AST-9877130, by the Department of Energy, through the PECASE and Scientific Discovery through Advanced Computing Programs, by funds from the Joint Institute for Heavy Ion Research, and by the Danish Research Council. Oak Ridge National Laboratory is managed by UT-Battelle, LLC, for the U.S. Department of Energy under Contract No. DE-AC05-00OR22725. G. M. P. acknowledges financial support of the Spanish MCyT under Contracts No. AYA2002-04094-C03-02 and No. AYA2003-06128.

[1] A. Burrows and J. M. Lattimer, Astrophys. J. **299**, L19 (1985).
[2] T. A. Thompson, A. Burrows, and P. A. Pinto, Astrophys. J. **592**, 434 (2003).
[3] A. Mezzacappa, M. Liebendörfer, O. Messer, W. Hix, F.-K. Thielemann, and S. Bruenn, Phys. Rev. Lett. **86**, 1935 (2001).
[4] M. Rampp and H.-T. Janka, Astrophys. J. **539**, L33 (2000).
[5] M. Liebendörfer, A. Mezzacappa, F.-K. Thielemann, O. E. B. Messer, W. R. Hix, and S.W. Bruenn, Phys. Rev. D **63**, 103004 (2001).
[6] J. R. Wilson and R.W. Mayle, Phys. Rep. **227**, 97 (1993).
[7] A. Burrows, J. Hayes, and B. A. Fryxell, Astrophys. J. **450**, 830 (1995).
[8] C. L. Fryer and M. S. Warren, Astrophys. J. **574**, L65 (2002).
[9] M. Herant, W. Benz, W. R. Hix, C. L. Fryer, and S. A. Colgate, Astrophys. J. **435**, 339 (1994).
[10] H.-T. Janka and E. Müller, Astron. Astrophys. **306**, 167 (1996).
[11] A. Mezzacappa, A. C. Calder, S.W. Bruenn, J. M. Blondin, M.W. Guidry, M. R. Strayer, and A. S. Umar, Astrophys. J. **493**, 848 (1998); **495**, 911 (1998).
[12] R. Buras, M. Rampp, H.-T. Janka, and K. Kifonidis, Phys. Rev. Lett. **90**, 241101 (2003).
[13] W. R. Hix and F.-K. Thielemann, Astrophys. J. **511**, 862 (1999).
[14] S. E. Woosley, in *16th Saas Fee Advanced Course, Nucleosynthesis and Chemical Evolution*, edited by B. Houck, A. Maeder, and G. Meynet (Geneva Observatory, Sauverny, 1986), pp. 1–193.
[15] J. Lattimer and F. D. Swesty, Nucl. Phys. **A535**, 331 (1991).
[16] M. Liebendörfer, O. E. B. Messer, A. Mezzacappa, and W. R. Hix, in *Proceedings of the 20th Texas Symposium on Relativistic Astrophysics*, edited by J. Wheeler and H. Martel (American Insitute of Physics, Melville, 2001), pp. 472–477.
[17] S.W. Bruenn, Astrophys. J. Suppl. Ser. **58**, 771 (1985).
[18] H. A. Bethe, G. E. Brown, J. Applegate, and J. M. Lattimer, Nucl. Phys. **A324**, 487 (1979).
[19] K. Langanke, G. Martinez-Pinedo, J. M. Sampaio, D. J. Dean, W. R. Hix, O. E. B. Messer, A. Mezzacappa, M. Liebendoerfer, H.-T. Janka, and M. Rampp, Phys. Rev. Lett. **90**, 241102 (2003).
[20] K. Langanke and G. Martínez-Pinedo, Nucl. Phys. A **673**, 481 (2000).
[21] K. Langanke, E. Kolbe, and D. J. Dean, Phys. Rev. C **63**, 032801 (2001).
[22] K. Langanke, G. Martínez-Pinedo, and J. M. Sampaio, Phys. Rev. C **64**, 055801 (2001).
[23] E. Bravo and D. García-Senz, Mon. Not. R. Astron. Soc. **307**, 984 (1999).
[24] W. R. Hix, Ph.D. thesis, Harvard University, 1995.
[25] M. F. El Eid and W. Hillebrandt, Astron. Astrophys. Suppl. Ser. **42**, 215 (1980).
[26] F. Brachwitz, D. Dean, W. Hix, K. Iwamoto, K. Langanke, G. Martinez-Pinedo, K. Nomoto, M. R. Strayer, and F.-K. Thielemann, Astrophys. J. **536**, 934 (2000).
[27] W. R. Hix, O. E. B. Messer, A. Mezzacappa, J. Sampaio, K. Langanke, D. J. Dean, and G. Martínez-Pinedo (to be published).
[28] A. Heger, K. Langanke, G. Martínez-Pinedo, and S. E. Woosley, Phys. Rev. Lett. **86**, 1678 (2001).
[29] G. M. Fuller, W. A. Fowler, and M. J. Newman, Astrophys. J. **293**, 1 (1985).
[30] A. Yahil, Astrophys. J. **265**, 1047 (1983).
[31] J. Pruet and G. M. Fuller, Astrophys. J. Suppl. Ser. **149**, 189 (2003).